Transforming a Fragile Protein Helix into an Ultrastable Scaffold via a Hierarchical AI and Chemistry Framework

Jun Qiu, Guojin Tang, Tianfu Feng, Bin Zheng, Yuanhao Liu, and Peng Zheng*

State Key Laboratory of Coordination Chemistry, Chemistry and Biomedicine Innovation Center (ChemBIC), School of Chemistry and Chemical Engineering, Frontier Interdisciplinary Science Research Center, Nanjing University; Nanjing, 210023, China.

*Corresponding author. Email: pengz@nju.edu.cn

Abstract: The rational design of proteins that maintain structural integrity under concurrent thermal, mechanical, and chemical stress remains a central challenge in molecular engineering. We present a hierarchical framework that transforms a fragile α-helical domain into an ultrastable scaffold by integrating AI-guided design with foundational chemical principles. This approach progresses from global architectural reinforcement, using multiple AI tools to create a stabilized four-helix bundle, to local chemical tuning, where AlphaFold3 guides the installation of salt bridges and metal-coordination motifs. A computational pipeline leveraging physics-based screening such as molecular dynamics (MD) simulations efficiently distilled millions of designs into a minimal candidate set. The resulting proteins exhibit unprecedented multi-axis stability, with mechanical unfolding forces exceeding 200 pN, thermal resilience >100 °C, and high resistance to chemical denaturants. By systematically dissecting the contributions of hydrophobic packing, electrostatics, and metal coordination, we establish a general blueprint for imparting extreme robustness. This work bridges AI-driven structural generation with chemical precision, advancing the creation of durable proteins for mechanistic studies and synthetic biology.

Introduction

Proteins that maintain their structural integrity when heated, stretched, or exposed to harsh solvents are foundational to both life[1-3] and serve as invaluable building blocks for advanced biomaterials[4-6], molecular devices[7,8], and operations in extreme environments[9,10]. Among natural scaffolds, helical architectures are particularly appealing targets due to their ubiquity and mechanical functionality: coiled-coils contribute to muscle and other cytoskeletal assemblies[11,12], talin rod domains act as mechanosensors that unfold under load[13-15], and arrays of α-helical bundles underlie the erythrocyte membrane skeleton[16-18]. These precedents motivate the goal of transforming common α-helical folds into programmable components with superior, multi-axis stability for diverse applications.

However, the rational design of such multi-faceted stability into isolated helical domains remains challenging[19]. The inherent mechanical fragility of the α-helix is a fundamental limitation; under tensile load, its hydrogen bonds rupture sequentially, leading to low unfolding forces of just tens of piconewtons (pN)[20-26], well below the hundreds of pN reached by mechanically robust β-sheet topologies pulled in shear[27]. This inherent fragility persists even in the presence of stable hydrophobic cores[28-34].

While decades of research have identified key chemical determinants of protein stability like hydrophobic packing, electrostatics, and metal coordination, with both natural and engineered examples showing these factors can enhance resilience[35-41], progress in increasing mechanical strength of isolate helical proteins has been a meaningful yet incremental process[42,43]. For example, only a few natural coiled-coils (e.g., in fibrinogen) approach 100 pN, while canonical α-helical bundles such as spectrin and ankyrin repeats typically unfold near 50 pN under comparable loading. The key challenge we address is thus to move beyond adding individual stabilizing features, and instead to precisely combine these different chemical interactions within a single architecture so they work together to resist multiple forms of stress.

The recent rise of generative AI for protein design has dramatically expanded the accessible fold space[44-48], offering a path to overcome the architectural limitations of natural scaffolds. However, a critical gap persists. AI models excel at global structure generation but often lack the understanding of local chemical interaction networks required for extreme, multi-axis stability. These models generate vast candidate libraries, creating a screening bottleneck that impedes the experimental validation essential for iterative, chemically rational design. A method that seamlessly integrates generative design with highly efficient screening is needed to bridge this gap.

Here, we treat multi-axis protein stabilization as a problem of hierarchical chemical engineering. We introduce an AI-guided blueprint that progresses systematically from global architectural reinforcement to atomistically precise chemical installation. First, AI-enabled backbone construction generates stable scaffolds with optimized hydrophobic cores, establishing a foundational stability layer. We then apply precision functionalization, installing a minimal set of inter-helical salt bridges and bi-histidine metal-coordination motifs through rational, site-specific edits.

This stepwise approach allows us to quantitatively dissect the mechanical contribution of each engineered chemical interaction[48].

To make this hierarchical chemical design tractable, we implement a computational pipeline that leverages developability filters[49], foldability assessment[44,47], and critically molecular dynamics (MD) simulations[50-52] to rank candidates based on proxies for mechanical and thermal resilience. This pipeline compresses ~10^6 *in silico* designs to a manageable number for experimental validation. The result is a family of ultrastable α-helical proteins where we can quantitatively attribute stability gains to specific chemical engineering steps: hydrophobic core optimization, electrostatic interaction, and metal-coordination clamping. This work provides a general, rational blueprint for the precision engineering of protein energy landscapes, transforming a mechanically weak architecture into a durable platform.

Results

Hierarchical design of ultrastable proteins by integrating AI and chemical principles

To establish a framework for programming multi-axis stability, we developed a hierarchical design strategy that integrates architectural and chemical stabilization principles. We selected the human spectrin repeat R15 (PDB code: 3F57)[53], a three-helix bundle that unfolds at ~50 pN and melts near 50 °C, as our design template (Fig. 1a-b). These moderate baseline properties provide an ideal starting point for quantitatively evaluating the contribution of each engineered stabilization layer. Our approach comprises two distinct stages (Fig. 1c): Stage I establishes a stabilized architectural framework through AI-guided backbone construction and computational screening, while Stage II applies precision functionalization with site-specific salt bridges and metal-coordination motifs to reinforce key structural interfaces.

In Stage I, we expanded the native architecture by appending a fourth helix to the spectrin template using RFdiffusion (Fig. 1d)[46]. We generated 100 backbone variants (50 each for N- and C-terminal extensions) and selected five optimal four-helix scaffolds based on bundle geometry, helical registry, and the potential for hydrophobic core densification without steric clash[54]. For each selected scaffold, we used ProteinMPNN to generate 100,000 sequences optimized for the remodeled core, producing a total library of 5×10^5 candidate sequences.[55]

To identify the best designs fulfilling our stability criteria, we implemented a multi-stage computational funnel that progresses from coarse filtering to high-fidelity functional prediction (Fig. 1e). The library was first subjected to a developability screen using physicochemical criteria (GRAVY < -0.3), retaining about 300,000 sequences with high predicted solubility and yield. Foldability was then assessed through a two-tiered model: ESMFold provided an initial screening to 357 designs, which were subsequently refined with AlphaFold2 under strict confidence thresholds

(pLDDT > 90, RMSD < 2.0 Å). This process yielded 211 high-confidence designs for further analysis.

Structural characterization revealed that the designed proteins exhibited enhanced packing, with a lower relative solvent-accessible surface area[56] (rSASA ≈ 0.35) compared to the natural spectrin repeat (rSASA ≈ 0.40). This was further supported by a higher proportion of residues with rSASA < 0.2 (designs: >30% vs. natural spectrin: 23%, see Raw Data 1), indicating successful hydrophobic core optimization[56].

We then implemented MD simulations to prioritize candidates based on functional stability metrics. Steered MD (SMD) simulations served as a mechanical proxy, stretching each domain under constant-velocity pulling to obtain relative stability rankings (Fig. 1b)[57]. Complementary annealing MD (AMD) simulations assessed thermal resilience through temperature ramping (310 K to 473 K) while monitoring structural integrity. These physics-based simulations provided the discriminatory power necessary to select candidates exhibiting target multi-axis stability. By integrating SMD and AMD results, we selected a final experimental shortlist that balances predicted mechanical and thermal resilience.

From this refined set, three variants, originally designated SpecAI87788, SpecAI16941, and SpecAI95889 (Fig. S1) based on their AI-generated identifiers, were selected for experimental validation based on their superior combined SMD and AMD performance (Fig. S2 and S3, Videos S1-S8). For clarity in subsequent analyses, these were renamed SpecAI88, SpecAI41, and SpecAI89, reflecting the last two digits of their original IDs.

The funnel compressed ~10^6 AI-generated sequences to 3 best candidates, preserving both scaffold and sequence diversity while prioritizing top performers. This selection process demonstrates how computational methods can efficiently navigate vast design spaces to identify optimal candidates for experimental characterization.

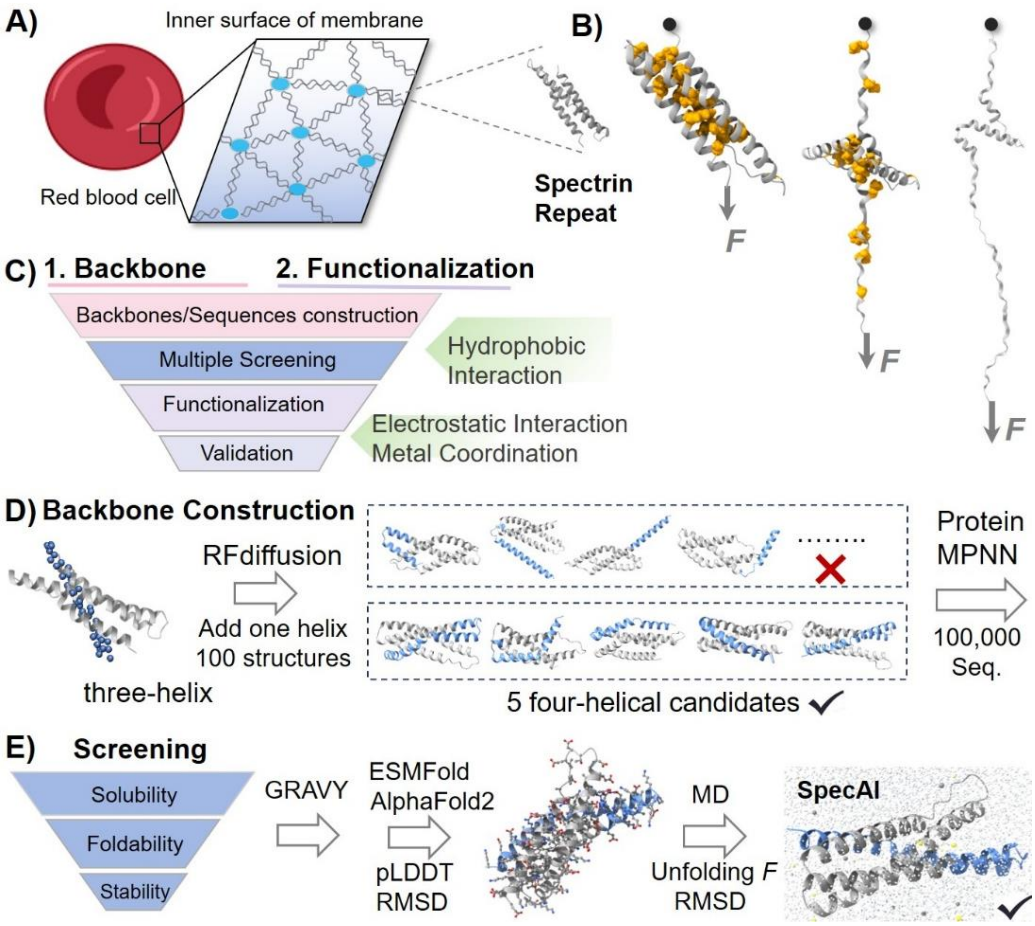

Fig. 1. A hierarchical chemical blueprint for multi-axis stabilization of α-helical protein. a, The erythrocyte membrane skeleton, which relies on spectrin repeats to withstand shear stress. Inset: Structure of a single, naturally fragile spectrin repeat (PDB 3F57), with hydrophobic core residues shown. **b,** The mechanical unfolding pathway of a spectrin repeat under tensile force, probed computationally by steered molecular dynamics (SMD) to generate force-extension curves. **c,** Overview of the two-stage design strategy. Stage I (Architectural Stabilization): AI-guided backbone construction and computational screening generate four-helix designs with optimized hydrophobic cores. Stage II (Precision Functionalization): Rational installation of inter-helical salt bridges and metal-coordination motifs reinforces specific mechanical interfaces. **d,** Stage I, Backbone construction. RFdiffusion appends a fourth helix to the native three-helix template, generating 100 initial backbones. Five optimal four-helix scaffolds are selected, and ProteinMPNN is used to generate 100,000 sequences per scaffold. **e,** Stage I, Computational screening. A multi-step funnel prioritizes candidates through successive filters: developability (GRAVY score ≤ -0.3), foldability (ESMFold triage followed by AlphaFold2 refinement with RMSD $\leq$ 2.0 Å and pLDDT $\geq$ 90), and stability assessed via molecular dynamics. The process efficiently narrows ~10^6 initial designs to an experimentally tractable shortlist.

Experimental verification of multi-axis stability in designed proteins

From the computational shortlist, we selected three representative designs, SpecAI88, SpecAI41, and SpecAI89, for experimental validation. All three expressed soluble in *E. coli* with high yields (~500 mg/L in TB, Table 1). SDS-PAGE showed the expected band near 19 *k*Da (Fig. S4), and mass spectroscopy confirmed molecular weights of 19,760, 19,108 and 19,285 Da, respectively (Fig. 2a). Far-UV circular dichroism (CD) spectroscopy was performed, revealing that all three proteins adopted predominantly α-helical structures, as indicated by the characteristic double minima at 208 nm and 222 nm (Fig. 2b)[58].

To evaluate thermal stability, we performed temperature-dependent circular dichroism (CD) measurements from 20°C to 100°C. All three designed proteins maintained substantial helical structure at 100°C, as evidenced by the retention of characteristic ellipticity at 195 nm, demonstrating exceptional thermodynamic stability (Fig. 2b, inset). We further challenged the proteins by performing thermal denaturation in the presence of the chemical denaturant guanidine hydrochloride (GdnHCl)[59]. Notably, all designs preserved their secondary structure at denaturant concentrations up to 3 M and maintained significant helical content under elevated temperature conditions (~50°C, 222 nm), demonstrating remarkable resistance to combined chaotropic stress (Fig. 2c). These results confirm not only the proper folding of these monomeric α-helical scaffolds but also validate that our Stage I designs, featuring optimized hydrophobic cores, achieve exceptional stability against both thermal and chemical denaturation.

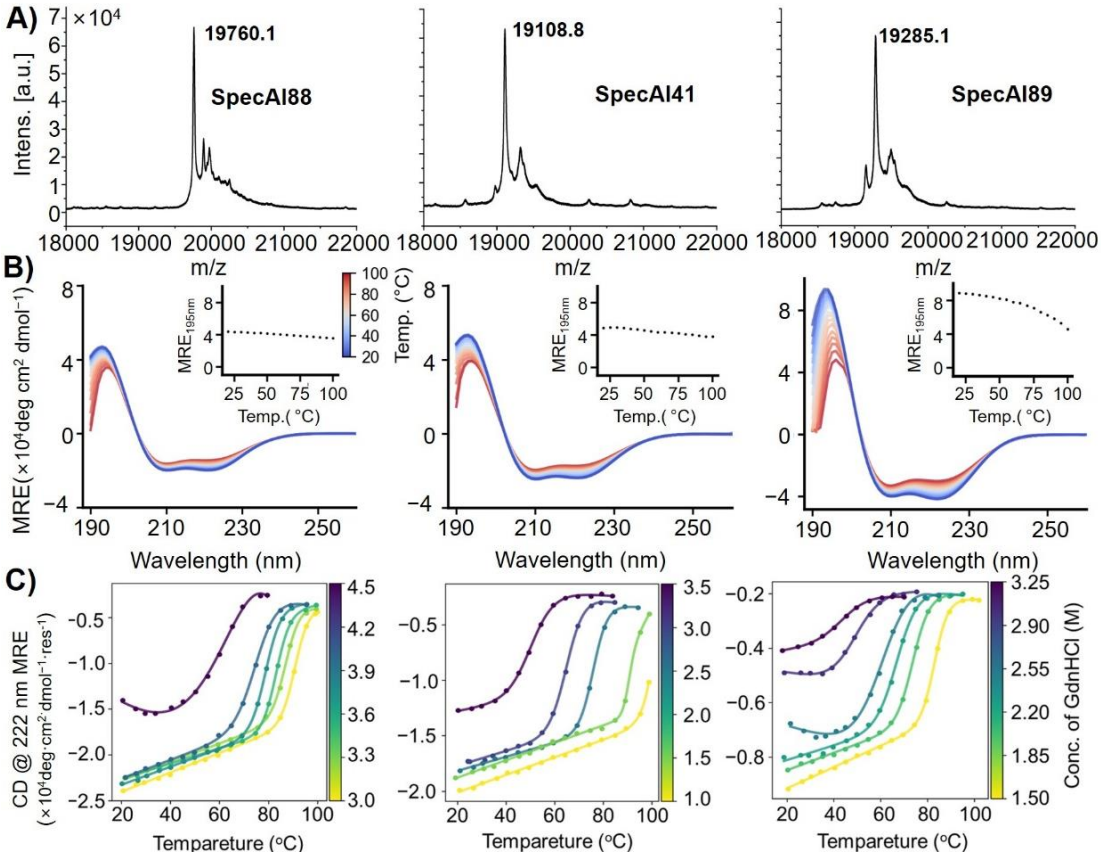

Fig. 2. Thermal and chemical robustness of AI-designed spectrin variants. a, MALDI-TOF mass spectrometry confirm molecular weights for SpecAI88, SpecAI41, and SpecAI89. **b,** Far-UV circular dichroism (190–260 nm) shows α-helical signatures with minima at 208 and 222 nm. Temperature-dependent CD (20–100 °C, blue to red) indicates substantial retention of ellipticity at 195 nm, with melting temperatures exceeding 100 °C. **c,** CD at 222 nm recorded in guanidinium chloride (GdnHCl) demonstrates persistence of α-helical signal at high denaturant concentrations (~3 M), indicating high chemical resistance.

Next, we directly quantified their mechanical stability using atomic force microscopy-based single-molecule force spectroscopy (AFM–SMFS). Each designed SpecAI domain was fused in series with three GB1 fingerprint domains and pulled via the high-strength Coh–Doc handle (rupture force ~400 pN), enabling unambiguous single-molecule identification (Fig. 3a)[60-62]. All experiments were conducted in a standard buffer at a pulling speed of 1000 nm/s unless otherwise specified. Force-extension curves were fitted with the worm-like chain (WLC) model to determine the contour length increment (ΔLc) for each unfolding event[63].

As expected, the natural spectrin control (102 amino acids in length) exhibited a ΔLc of 32 nm, in addition to the unfolding steps of the three GB1 domains (18 nm each)[64]. In contrast, the designed SpecAI proteins showed a significantly larger ΔLc of ≈52 nm (Fig. 3b, Fig. S1), consistent with the full unraveling of their ~150-residue domain. The measured values: 52 ± 2 nm (SpecAI88), 53 ± 1 nm (SpecAI41), and 52 ± 2 nm (SpecAI89) (mean ± s.e.m., from Gaussian fit), closely matched theoretical predictions, thereby confirming the correct assignment of the designed domain's unfolding (Fig. 3c).

Most importantly, all three SpecAI variants exhibited markedly elevated unfolding forces compared to natural spectrin (56 ± 3 pN; n=212). The average unfolding forces reached 116 ± 2 pN (SpecAI88; n=224), 156 ± 4 pN (SpecAI41; n=218), and 121 ± 4 pN (SpecAI89; n=174) (Fig. 3c, Table 1). The combination of accurate ΔLc, the presence of three GB1 fingerprint domains, and consistent force statistics confirms single-molecule specificity and establishes a new mechanical baseline for α-helical proteins created through Stage I backbone design.

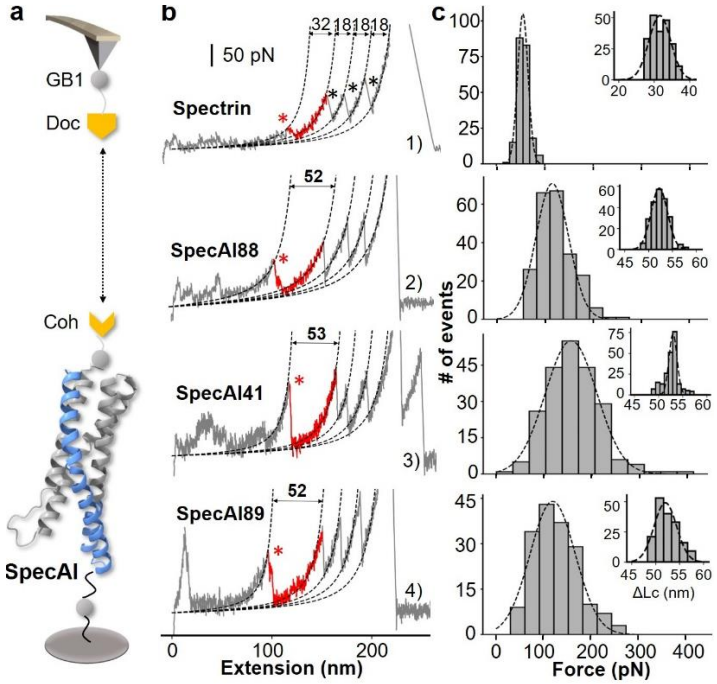

Fig. 3. Stage I four-helix bundle designs exhibit enhanced mechanical stability by single-molecule force spectroscopy. a, Schematic of the AFM–SMFS experimental setup. A dockerin (Doc)-functionalized AFM tip engages a cohesin (Coh)-tagged SpecAI construct immobilized on the surface, enabling single-molecule pulling. The construct includes three GB1 domains as fingerprint markers. **b,** Representative force-extension curves. Curve 1: Unfolding of the natural spectrin repeat (ΔLc ≈ 32 nm, red), followed by three GB1 (ΔLc ≈ 18 nm per domain, black). Curves 2-4: Unfolding of SpecAI variants (ΔLc ≈ 53 nm). Sometimes, the Doc unfolds showing additional peak (Curve 3). Dashed lines are worm-like chain model fit. **c,** Unfolding force histograms of SpecAI (bin size= 30 pN) with Gaussian fits demonstrate a significant increase in mechanical stability compared to the native spectrin repeat (56 ± 3 pN, n = 212, bin size=13.75 pN): SpecAI88, 116 ± 2 pN (n = 224); SpecAI41, 156 ± 4 pN (n = 218) and SpecAI89, 121 ± 4 pN (n = 174). The corresponding ΔLc distributions are centered near 52 nm, consistent with the full unfolding of the designed domain.

Table 1. Stability of AI-designed spectrin with four α-helices

Protein	SMD (pN) 1 nm/ns	*Tm* (°C)	Yield (mg/L)	AFM (pN)	ΔLc (nm)	Δ*F* (pN)
Spectrin	599±62	~50	~50	56 ± 3	32 ± 1	N/A
SpecAI88	735±80	>100	580 ± 36	116 ± 2	52 ± 2	60
SpecAI41	689±84	>100	625 ± 28	156 ± 4	53 ± 1	100
SpecAI89	670±84	>100	450 ± 16	121 ± 4	52 ± 2	61

Values for SMD are reported as mean ± SD, while all other values are reported as

Gaussian fit mean ± s.e.m. ΔF means the unfolding force increase over spectrin.

Precision scaffold functionalization via hierarchical chemical design

Building upon the stabilized architectural frameworks from Stage I, we implemented a precision functionalization strategy to further enhance stability through the rational design of specific chemical interactions at inter-helical interfaces. This stage involved two complementary approaches: engineering of electrostatic salt bridges and incorporation of metal-coordination motifs (Fig. 4a).

Our design strategy followed a rigorous hierarchical selection process. First, we identified potential mutation sites by excluding residues critical for hydrophobic core integrity, focusing instead on positions at inter-helical interfaces that could accommodate new interactions without perturbing the existing structural stability. Second, we employed AlphaFold3 (AF3) structure prediction to evaluate potential mutations, requiring that designs not only maintain high overall structural confidence (pLDDT > 80 for all mutated residues, with many exceeding 90 but also satisfy precise geometric criteria for the intended molecular interactions, specifically in terms of inter-atomic distances.

We designed and incorporated single inter-helical salt bridges into each optimized parent scaffold: SpecAI41-9K152D (Fig. 4b, Fig. S1), SpecAI88-49E102K, and SpecAI89-25E48K (Fig. S7). AF3 models confirmed that the engineered residues were positioned at interface-facing turns with favorable i↔i' or i±1 helical register arrangements without introducing steric clashes. Crucially, all designed salt bridges showed charged atom distances <0.4 nm in the predicted structures, and the contacts remained stable following backbone relaxation simulations. This consistency indicates genuine local interface reinforcement rather than global structural reorganization. All mutated backbone atoms maintained high pLDDT scores (>80), confirming the preservation of structural integrity. For example, the pLDDT scores for the Cα atoms were 90.1 and 80.7 for SpecAI41-9K152D.

AFM-SMFS measurements revealed ~30 pN increases relative to Stage-I parents with ΔLc unchanged (~53 nm), as expected. Unfolding forces were 180 ± 4 pN (n = 197) for SpecAI41-9K152D (Fig. 4c–d), 141 ± 3 pN (n = 202) for SpecAI88-49E102K, and 153 ± 4 pN (n = 264) for SpecAI89-25E48K (Fig. S7, Table 2). The constant ΔLc across parents and salt-bridge variants indicates that electrostatic installation does not change topology or domain length, but raises the mechanical barrier along the established pathway.

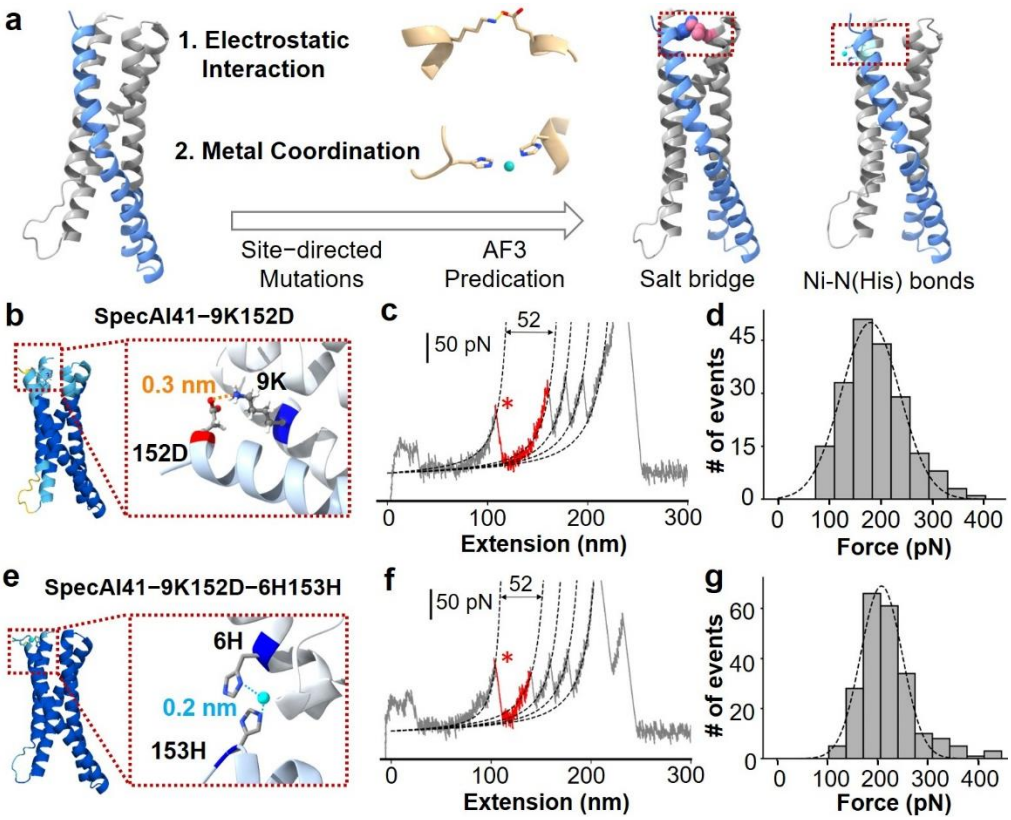

Fig. 4. Precision stabilization of designed proteins via electrostatic interactions and metal coordination. a Schematic of Stage II design: introducing inter-helical ion pairs and metal-coordination sites into AI-designed backbones to stabilize specific interfaces. **b,** AlphaFold3-predicted structure of variant SpecAI41-9K152D, showing an engineered salt bridge (Lys9-Asp152, 3 Å) designed for electrostatic stabilization without perturbing the core. The color of protein is based on the pLDDT value, showing a high confidence structure prediction (>80). **c,** A representative force-extension curve for the salt-bridge variant shows an unfolding event with a ΔLc of 53 nm, consistent with the parent scaffold. **d,** Unfolding force histograms reveal a ~25 pN increase in mechanical stability for salt-bridge variants compared to their Stage-I parents. **e,** Introduction of a metal-binding site in variant SpecAI41-9K152D-6H153H, with two histidines positioned 2 Å apart, compatible with Ni^{2+} coordination. **f,** A representative force-extension curve recorded in 200 μM Ni^{2+} shows the unfolding event (ΔLc ≈ 53 nm). **g,** Unfolding force histograms confirm enhanced mechanical stability, with forces reaching ~200 pN, a significant gain over the salt-bridge parent.

Table 2. SpecAI stability further enhanced by site-specific functionalization

Protein	Force (pN)	ΔLc (nm)	Δ*F* (pN)	Total ΔF
SpecAI88-49E102K	141 ± 3	54 ± 1	25	74
+6H149H	190 ± 3	53 ± 1	49	
SpecAI41-9K152D	180 ± 4	53 ± 2	24	52
+6H153H	208 ± 3	53 ± 2	28	
SpecAI89-25E48K	153 ± 4	53 ± 1	32	52

+24H135H	173 ± 3	53 ± 1	20	

Total ΔF means the unfolding force increase over SpecAI.

To achieve additional mechanical reinforcement, we designed bi-histidine motifs capable of forming intra-domain Ni(II)-coordination sites[63]. These motifs were strategically positioned on adjacent helices to create bidentate metal-binding pockets without perturbing the hydrophobic core. Our design criteria targeted Ni-N(His) distances of ~2.0 Å, Cα-Cα spacing compatible with inter-helical bridging rotamers, and proper side-chain orientation (Nδ1/Nε2) for optimal imidazole coordination geometry. This approach yielded three metal-coordination variants: SpecAI41-9K152D-6H153H, SpecAI88-49E102K-6H149H and SpecAI89-25E48K-24H135H (Fig. 4, Fig. S1&S7), whose structures were validated using AF3 again.

In the presence of 200 μM Ni^{2+}, AFM-SMFS revealed a further significant increase in mechanical stability over the salt-bridge parents, with unfolding forces reaching 208 ± 3 pN (n = 222) for SpecAI41-9K152D-6H153H, 190 ± 3 pN (n = 232) for SpecAI88-49E102K-6H149H, and 173 ± 3 pN (n = 204) for SpecAI89-25E48K-24H135H, and an unchanged ΔLc of ~53 nm (Table 2). These results are consistent with a short, inner-interface coordination clamp that reinforces the native unfolding pathway without introducing alternative topologies.

We further characterized the unfolding kinetics of the computationally designed proteins via dynamic force spectroscopy across a range of pulling speeds, focusing on the SpecAI41 series due to its highest unfolding force. The unfolding forces of the three SpecAI41 exhibited the expected linear dependence on the logarithm of the loading rate (Fig. S8). Fitting the data to the Bell-Evans model yielded a consistent distance to the transition state (Δx ≈0.19 nm) for all three constructs, while the spontaneous unfolding rate (k_{off}) decreased progressively from SpecAI41 (0.44 s^{-1}) to the salt-bridge (0.09 s^{-1}) and metal-coordination (0.05 s^{-1}) variants. This kinetic profile further confirms that the engineered stabilizations raise the activation barrier for unfolding without altering the unfolding pathway.

This hierarchical computational design methodology (Fig. 5), progressing from architectural stabilization to precision functionalization, enabled the predictable enhancement of protein stability through the additive contribution of distinct chemical interaction networks.

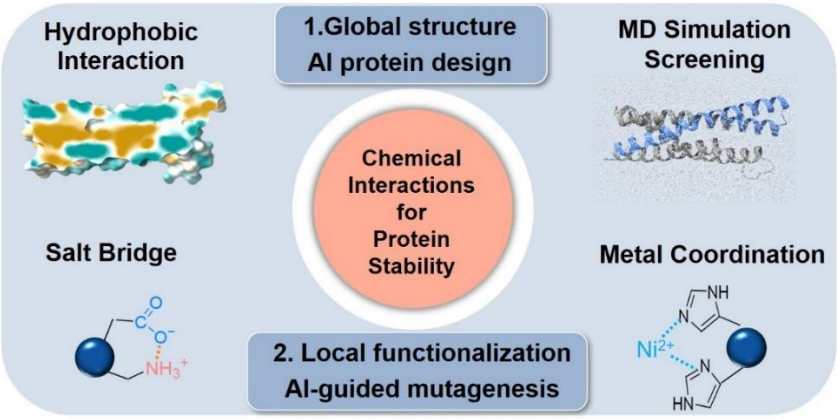

Fig. 5. Hierarchical computational design of ultrastable proteins through multi-scale stabilization. Schematic summarizing the two-stage design strategy for additive mechanical reinforcement. Stage I establishes a stable architectural framework through MD screening of AI-designed hydrophobically optimized cores. Stage II introduces precision functionalization via inter-helical salt bridges and bi-histidine metal-coordination motifs, guided by AlphaFold3 structural models. The integration of global architectural stability with local chemical cross-linking produces additive mechanical reinforcement, enabling the creation of ultrastable protein domains.

Discussion

The rational design of proteins capable of withstanding concurrent thermal, chemical, and mechanical stress remains a fundamental challenge. Here, we present a hierarchical strategy that integrates chemically distinct stabilization mechanisms within a single protein architecture. Our approach not only provides a robust blueprint for creating ultrastable proteins but also decouples the quantitative contributions of hydrophobic packing, electrostatic interactions, and metal coordination to mechanical resilience.

Our work builds upon established principles of α-helical protein stability while introducing substantive advances. Whereas most isolated α-helical domains unfold below 20 pN due to sequential hydrogen bond rupture[65], our designed variants achieve forces up to 200 pN. This represents a significant advance beyond canonical α-helical bundles such as spectrin and ankyrin repeats, which typically unfold near 50 pN[66]. Previous engineering strategies have demonstrated incremental improvements[42], but our contribution lies in the systematic integration of global architectural optimization with local chemical reinforcement within a unified design framework enabled by AI protein design and computational screening[67,68].

The hierarchical organization of our approach proved particularly effective. We first established a stable structural framework through computational design of an optimized hydrophobic core, providing baseline mechanical stability of ~120 pN. Subsequent precision functionalization with inter-helical salt bridges contributed an additional ~30 pN, while metal coordination sites provided further gains of ~50 pN

depending on geometric parameters. This modular strategy demonstrates that distinct chemical interaction networks can be engineered to operate additively within a single protein structure[69].

Notably, conventional structural metrics such as pLDDT scores, while predictive of foldability, show limited correlation with mechanical stability. This divergence underscores that dynamic functional properties require physics-based simulation. Although steered molecular dynamics (SMD) overestimates absolute unfolding forces due to computationally mandated high pulling speeds[70] (e.g., ~600 pN *in silico* versus ~50 pN for spectrin in experiment), it served as a powerful semi-quantitative screen. The strong agreement between computational rankings and experimental measurements validates this approach for prioritizing designs based on relative mechanostability, offering a practical pipeline to bridge the gap between *in silico* design and experimental validation.

Moreover, our computational pipeline addresses a critical challenge in modern protein design: efficiently transitioning from in silico designs to experimentally testable candidates. The multi-stage screening process, progressing from physicochemical properties to foldability and finally to functional stability assessments, significantly reduced experimental burden while maintaining high success rates, enhancing accessibility for research groups without extensive high-throughput capabilities.

In conclusion, our hierarchical framework provides a generalizable route to programming protein stability. By modular integration of architectural and chemical stabilization strategies, we can now tailor mechanical, thermal, and chemical resistance in α-helical proteins. This approach will accelerate the development of robust protein-based materials and molecular devices for demanding applications in biotechnology and synthetic biology[71,72].

Supplementary Information includes: supplementary methods, notes, figures S1-S8 and videos (1-8), providing additional experimental details such as protein expression and purification, AFM-SMFS system, MD simulations, and data analysis procedure.

Competing interests: The authors declare no competing interests.

Data availability statement: All data are present in the main text or supplementary information.

Acknowledgments: The numerical calculations in this work have been done on the computing facilities in the High-Performance Computing Center (HPCC) of Nanjing University. We thank the funding from Natural Science Foundation of China (22477058, 22588302), Fundamental Research Funds for the Central Universities (2025300302, KG202503), and Natural Science Foundation of Jiangsu Province (BK20202004). We also thank previous reviewers' comments that inspired this study.

Reference:

1 Rief, M., Gautel, M., Oesterhelt, F., Fernandez, J. M. & Gaub, H. E. Reversible unfolding of individual titin immunoglobulin domains by AFM. *Science* **276**, 1109-1112 (1997).

2 Manteca, A. *et al.* Mechanochemical evolution of the giant muscle protein titin as inferred from resurrected proteins. *Nat. Struct. Mol. Biol.* **24**, 652-657 (2017).

3 Neupane, K. *et al.* Direct observation of prion-like propagation of protein misfolding templated by pathogenic mutants. *Nat. Chem. Biol.* **20**, 1220-1226 (2024).

4 Sivasankaran, R. P. *et al.* Polymer-mediated protein/peptide therapeutic stabilization: Current progress and future directions. *Prog. Polym. Sci.* **156**, 101867 (2024).

5 Fu, L. *et al.* Cartilage-like protein hydrogels engineered via entanglement. *Nature* **618**, 740-747 (2023).

6 Miserez, A., Yu, J. & Mohammadi, P. Protein-Based Biological Materials: Molecular Design and Artificial Production. *Chem. Rev.* **123**, 2049-2111 (2023).

7 Yang, S. *et al.* DNA-functionalized artificial mechanoreceptor for de novo force-responsive signaling. *Nat. Chem. Biol.* **20**, 1066-1077 (2024).

8 Devaux, F. *et al.* Single-molecule mechanics of synthetic aromatic amide helices: Ultrafast and robust non-dissipative winding. *Chem* **7**, 1333-1346 (2021).

9 Bustamante, C., Chemla, Y. R., Forde, N. R. & Izhaky, D. Mechanical processes in biochemistry. *Annu. Rev. Biochem.* **73**, 705-748 (2004).

10 Pepelnjak, M. *et al.* In situ analysis of osmolyte mechanisms of proteome thermal stabilization. *Nat. Chem. Biol.* **20**, 1053-1065 (2024).

11 Schwaiger, I., Sattler, C., Hostetter, D. R. & Rief, M. The myosin coiled-coil is a truly elastic protein structure. *Nat. Mater.* **1**, 232-235 (2002).

12 Baumann, F. *et al.* Increasing evidence of mechanical force as a functional regulator in smooth muscle myosin light chain kinase. *Elife* **6**, e26473 (2017).

13 del Rio, A. *et al.* Stretching single talin rod molecules activates vinculin binding. *Science* **323**, 638-641 (2009).

14 Tapia-Rojo, R. *et al.* Enhanced statistical sampling reveals microscopic complexity in the talin mechanosensor folding energy landscape. *Nat. Phys.* **19**, 52-60 (2023).

15 Le, S., Yu, M. & Yan, J. Direct single-molecule quantification reveals unexpectedly high mechanical stability of vinculin-talin/alpha-catenin linkages. *Sci. Adv.* **5**, eaav2720 (2019).

16 Rief, M., Pascual, J., Saraste, M. & Gaub, H. E. Single molecule force spectroscopy of spectrin repeats: low unfolding forces in helix bundles. *J. Mol. Bio.* **286**, 553-561 (1999).

17 Takahashi, H., Rico, F., Chipot, C. & Scheuring, S. alpha-Helix Unwinding as

Force Buffer in Spectrins. *Acs Nano* **12**, 2719-2727 (2018).

18 Wensley, B. G. *et al.* Experimental evidence for a frustrated energy landscape in a three-helix-bundle protein family. *Nature* **463**, 685-688 (2010).

19 Baker, E. G. *et al.* Engineering protein stability with atomic precision in a monomeric miniprotein. *Nat. Chem. Biol.* **13**, 764-770 (2017).

20 Carrion-Vazquez, M. *et al.* Mechanical design of proteins-studied by single-molecule force spectroscopy and protein engineering. *Prog. Biophys. Mol. Biol.* **74**, 63-91 (2000).

21 LeBlanc, M. A., Fink, M. R., Perkins, T. T. & Sousa, M. C. Type III secretion system effector proteins are mechanically labile. *Proc. Natl. Acad. Sci. U. S. A.* **118**, e2019566118 (2021).

22 Hoffmann, T., Tych, K. M., Hughes, M. L., Brockwell, D. J. & Dougan, L. Towards design principles for determining the mechanical stability of proteins. *Phys. Chem. Chem. Phys.* **15**, 15767-15780 (2013).

23 Neuman, K. C. & Nagy, A. Single-molecule force spectroscopy: optical tweezers, magnetic tweezers and atomic force microscopy. *Nat. Methods* **5**, 491-505 (2008).

24 Muller, D. J. *et al.* Atomic Force Microscopy-Based Force Spectroscopy and Multiparametric Imaging of Biomolecular and Cellular Systems. *Chem. Rev.* **121**, 11701-11725 (2021).

25 Law, R. *et al.* Cooperativity in Forced Unfolding of Tandem Spectrin Repeats. *Biophys. J.* **84**, 533-544 (2003).

26 Randles, L. G., Rounsevell, R. W. S. & Clarke, J. Spectrin Domains Lose Cooperativity in Forced Unfolding. *Biophys. J.* **92**, 571-577 (2007).

27 Brockwell, D. J. *et al.* Pulling geometry defines the mechanical resistance of a beta-sheet protein. *Nat. Struct. Mol. Biol.* **10**, 731-737 (2003).

28 Collet, J.-P., Shuman, H., Ledger, R. E., Lee, S. & Weisel, J. W. The elasticity of an individual fibrin fiber in a clot. *Proc. Natl. Acad. Sci. U. S. A.* **102**, 9133-9137 (2005).

29 Lee, G. *et al.* Nanospring behaviour of ankyrin repeats. *Nature* **440**, 246-249 (2006).

30 Lim, B. B. C., Lee, E. H., Sotomayor, M. & Schulten, K. Molecular Basis of Fibrin Clot Elasticity. *Structure* **16**, 449-459 (2008).

31 Minin, K. A., Zhmurov, A., Marx, K. A., Purohit, P. K. & Barsegov, V. Dynamic Transition from α-Helices to β-Sheets in Polypeptide Coiled-Coil Motifs. *J. Am. Chem. Soc.* **139**, 16168-16177 (2017).

32 Milles, L. F., Bayer, E. A., Nash, M. A. & Gaub, H. E. Mechanical Stability of a High-Affinity Toxin Anchor from the Pathogen Clostridium perfringens. *J. Phys. Chem. B* **121**, 3620-3625 (2017).

33 Ng, S. P. *et al.* Designing an extracellular matrix protein with enhanced mechanical stability. *Proc. Natl. Acad. Sci. U. S. A.* **104**, 9633-9637 (2007).

34 Craig, D., Gao, M., Schulten, K. & Vogel, V. Tuning the Mechanical Stability

of Fibronectin Type III Modules through Sequence Variations. *Structure* **12**, 21-30 (2004).

35 Kellis, J. T., Nyberg, K., Sˇail, D. a. & Fersht, A. R. Contribution of hydrophobic interactions to protein stability. *Nature* **333**, 784-786 (1988).

36 Marqusee, S. & Baldwin, R. L. Helix stabilization by Glu-...Lys+ salt bridges in short peptides of de novo design. *Proc. Natl. Acad. Sci. U. S. A.* **84**, 8898-8902 (1987).

37 Baker, E. G. *et al.* Local and macroscopic electrostatic interactions in single α-helices. *Nat. Chem. Biol.* **11**, 221-228 (2015).

38 Goldenzweig, A. & Fleishman, S. J. Principles of Protein Stability and Their Application in Computational Design. *Annu. Rev. Biochem.* **87**, 105-129 (2018).

39 Wang, Z., Nie, J., Shi, S., Li, G. & Zheng, P. Transforming de novo protein a3D into a mechanically stable protein by zinc binding. *Chem. Commun.* **57**, 11489-11492 (2021).

40 Zhang, X., Zhang, H., Lu, S., Song, Y. & Zhang, W. Direct Detection of the Chain Trajectory and Long-Range Correlation in Crystalline–Amorphous Polymer Networks by Single-Molecule Force Spectroscopy. *Macromolecules* **58**, 6170-6177 (2025).

41 Nandi, T. & Ainavarapu, S. R. K. Native Salt Bridges Are a Key Regulator of Ubiquitin's Mechanical Stability. *J. Phys. Chem. B* **126**, 3505-3511 (2022).

42 Lopez-Garcia, P. *et al.* Fortified Coiled Coils: Enhancing Mechanical Stability with Lactam or Metal Staples. *Angew. Chem. Int. Ed.* **60**, 232-236 (2021).

43 Tunn, I., de Leon, A. S., Blank, K. G. & Harrington, M. J. Tuning coiled coil stability with histidine-metal coordination. *Nanoscale* **10**, 22725-22729 (2018).

44 Jumper, J. *et al.* Highly accurate protein structure prediction with AlphaFold. *Nature* **596**, 583-589 (2021).

45 Dauparas, J. *et al.* Robust deep learning–based protein sequence design using ProteinMPNN. *Science* **378**, 49-56 (2022).

46 Watson, J. L. *et al.* De novo design of protein structure and function with RFdiffusion. *Nature* **620**, 1089-1100 (2023).

47 Lin, Z. *et al.* Evolutionary-scale prediction of atomic-level protein structure with a language model. *Science* **379**, 1123-1130 (2023).

48 Sakuma, K. *et al.* Design of complicated all-α protein structures. *Nat. Struct. Mol. Biol.* **31**, 275-282 (2024).

49 Kyte, J. & Doolittle, R. F. A simple method for displaying the hydropathic character of a protein. *J. Mol. Bio.* **157**, 105-132 (1982).

50 Karplus, M. & McCammon, J. A. Molecular dynamics simulations of biomolecules. *Nat. Struct. Biol.* **9**, 646-652 (2002).

51 Milles, L. F., Schulten, K., Gaub, H. E. & Bernardi, R. C. Molecular mechanism of extreme mechanostability in a pathogen adhesin. *Science* **359**,

1527-1533 (2018).
52 Rennekamp, B., Grubmüller, H. & Gräter, F. Hidden length lets collagen buffer mechanical and chemical stress. *Phys. Rev. E* **110**, 054408 (2024).
53 Ipsaro, J. J., Huang, L. & Mondragón, A. Structures of the spectrin-ankyrin interaction binding domains. *Blood* **113**, 5385-5393 (2009).
54 Lombardi, A., Pirro, F., Maglio, O., Chino, M. & DeGrado, W. F. De Novo Design of Four-Helix Bundle Metalloproteins: One Scaffold, Diverse Reactivities. *Acc. Chem. Res.* **52**, 1148-1159 (2019).
55 Liu, L. *et al.* De Novo Design Mechanostable Titin Ig Domain Using Artificial Intelligence and Steered Molecular Dynamics Simulations. *CCS Chem.* **7**, 1629-1640 (2025).
56 Porollo, A. *et al.* Maximum Allowed Solvent Accessibilites of Residues in Proteins. *PLoS ONE* **8,** e80635 (2013).
57 Ni, B., Kaplan, D. L. & Buehler, M. J. ForceGen: End-to-end de novo protein generation based on nonlinear mechanical unfolding responses using a language diffusion model. *Sci. Adv.* **10**, eadl4000 (2024).
58 Greenfield, N. J. Using circular dichroism spectra to estimate protein secondary structure. *Nat. Protoc.* **1**, 2876-2890 (2007).
59 Liu, Z. & Thirumalai, D. Impact of Guanidinium Hydrochloride on the Shapes of Prothymosin-α and α-Synuclein Is Dramatically Different. *Biochemistry-Us* **64**, 105-113 (2025).
60 Stahl, S. W. *et al.* Single-molecule dissection of the high-affinity cohesin-dockerin complex. *Proc. Natl. Acad. Sci. U. S. A.* **109**, 20431-20436 (2012).
61 Deng, Y. *et al.* Enzymatic biosynthesis and immobilization of polyprotein verified at the single-molecule level. *Nat. Commun.* **10**, 2775-2785 (2019).
62 Shi, S. *et al.* Combination of Click Chemistry and Enzymatic Ligation for Stable and Efficient Protein Immobilization for Single-Molecule Force Spectroscopy. *CCS Chem.* **4**, 598-604 (2022).
63 Marko, J. F. & Siggia, E. D. Stretching DNA. *Macromolecules* **28**, 8759-8770 (1995).
64 Cao, Y., Lam, C., Wang, M. & Li, H. Nonmechanical protein can have significant mechanical stability. *Angew. Chem. Int. Ed.* **45**, 642-645 (2006).
65 Wolny, M. *et al.* Stable Single α-Helices Are Constant Force Springs in Proteins. *J. Bio. Chem.* **289**, 27825-27835 (2014).
66 Serquera, D. *et al.* Mechanical Unfolding of an Ankyrin Repeat Protein. *Biophys. J.* **98**, 1294-1301 (2010).
67 Thomas, A. S. & Elcock, A. H. Molecular Simulations Suggest Protein Salt Bridges Are Uniquely Suited to Life at High Temperatures. *J. Am. Chem. Soc.* **126**, 2208-2214 (2004).
68 Wolny, M. *et al.* Characterization of long and stable de novo single alpha-helix domains provides novel insight into their stability. *Sci. Rep.* **7**, 44341 (2017).

69 Cao, Y., Li, Y. D. & Li, H. Enhancing the mechanical stability of proteins through a cocktail approach. *Biophys. J.* **100**, 1794-1799 (2011).

70 Merkel, R., Nassoy, P., Leung, A., Ritchie, K. & Evans, E. Energy landscapes of receptor-ligand bonds explored with dynamic force spectroscopy. *Nature* **397**, 50-53 (1999).

71 Ling, S., Kaplan, D. L. & Buehler, M. J. Nanofibrils in nature and materials engineering. *Nat. Rev. Mater.* **3**, 18016-18035 (2018).

72 Klein, D. & Nanda, V. The proteins that could be. *Nat. Rev. Chem.* **9**, 283-284 (2025).